

## Biophysics in reverse: Using blood cells to accurately calibrate force-microscopy cantilevers

Volkmar Heinrich<sup>a)</sup> and Chawin Ounkomol

Department of Biomedical Engineering and Biomedical Engineering Graduate Group, University of California, Davis, 451 Health Sciences Drive, Davis, California 95616, USA

(Received 5 February 2008; accepted 25 March 2008; published online 16 April 2008)

We report on the refinement and validation of one of the earliest ideas of “reverse” biophysics: the use of individual red blood cells as reliable, ultrasensitive mechanotransducers. Our analysis is based on the numerical prediction of the force exerted by a micropipette-held red cell as it is pushed against a test object. Examining this red-cell transducer, in conjunction with a custom-built “horizontal” force microscope, we were able to soundly corroborate its utility, while at the same time, accurately calibrating the spring constants of atomic-force microscope cantilevers.

© 2008 American Institute of Physics. [DOI: 10.1063/1.2909529]

Foremost among the special rules that apply when one studies or tries to mimic nanoscale biology is that even minuscule mechanical forces may dramatically impact molecular and cellular behavior. This corollary of dynamic force spectroscopy<sup>1</sup> originates from the *exponential* dependence of the dissociation rates of “weak” interactions (which are governed by energies comparable to the thermal energy scale  $k_B T$ ) on force.<sup>2</sup> Most molecular-to-cellular processes indeed involve some form of stress-bearing, weak interactions. Understanding how they are affected by force is, therefore, a central part of rigorous nanobioscience and technology. It requires not only expanding the available tool chest of nanoscale biophysics but also ensuring the highest possible accuracy of the force probes in use.<sup>3</sup>

The present study tests two such force probes against one another: a commercially available cantilever commonly used in atomic-force microscopes<sup>4</sup> (AFM) and a pipette-pressurized red blood cell.<sup>5–7</sup> Recent progress on two fronts has made this study possible. First, our numerical treatment of the mechanical equilibrium of an axially stressed, pipette-aspirated closed membrane<sup>8</sup> provides an accurate prediction of the force-deflection behavior of the red-cell transducer under compression. Second, by turning the core components of conventional AFMs on the side, our custom-built “horizontal AFM”<sup>9</sup> allows us to combine the exquisite spatial and temporal resolution of the AFM with optical microscopy and with the enormous versatility provided by an automated micropipette-manipulation setup (Fig. 1).<sup>10</sup>

A pipette-pressurized red blood cell is probably the most readily available transducer to apply and measure piconewton forces. The only requirements for a red cell to reliably operate as an ultrasensitive force probe are a fluid membrane and cell interior, reasonable lubrication between the membrane and pipette wall, and at least a moderate aspiration pressure. Beside its low cost, a unique advantage of the red-cell transducer is that its probe stiffness can be calculated from first principles and is *tunable* via the pipette-aspiration pressure. The underlying analysis assumes that the transducer’s force-deflection relationship is largely independent of the constitutive behavior of individual cells—an assumption

whose verification is one of the goals of this study. At the same time, as we ascertain the utility of the red cell as a viable nanomechanical tool, we use it to determine the spring constant of the AFM cantilever against which the red cells are tested.

Figure 1 illustrates the straightforward experimental procedure. A preswollen red blood cell is aspirated in a custom-made micropipette with a well-calibrated suction pressure. It is then maneuvered close to the tip of a rectangular AFM cantilever. The cantilever, a diode laser, and a position detector are arranged in a horizontal configuration on the stage of an inverted optical microscope, providing the cantilever deflection with nanometer resolution and at sampling frequencies up to 1 MHz using the “optical-lever” approach.<sup>11,12</sup> A

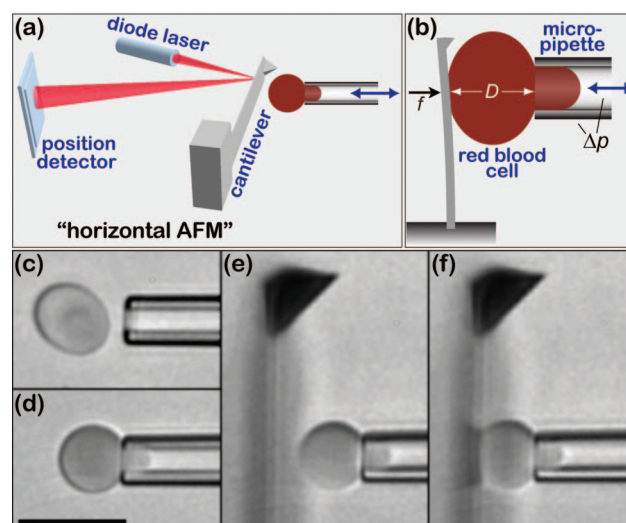


FIG. 1. (Color) Overview of the experimental setup and procedure. [(a) and (b)] The core components of the horizontal AFM are arranged perpendicular to the optical axis of an inverted microscope, providing a side view of the cantilever and allowing for easy integration of a micropipette setup. The double arrow denotes pipette translation to/from the cantilever by closed-loop piezoactuation. (The sketches are not to scale.) [(c)–(f)] Videomicrographs (bar = 10  $\mu\text{m}$ ) show how a preswollen (at  $\sim 150$  mOsm) red blood cell is first picked up in a pipette (cylindrical tip, ID  $\sim 2.2$   $\mu\text{m}$  [(c) and (d)]), then manipulated close to the tip of the cantilever (e), and repeatedly pushed against the flat of the cantilever (f). (The side view of the  $\sim 30$ - $\mu\text{m}$ -wide cantilever creates a blurry diffraction pattern; only the cantilever tip appears more or less in focus.)

<sup>a)</sup> Author to whom correspondence should be addressed. Electronic mail: vheinrich@ucdavis.edu.

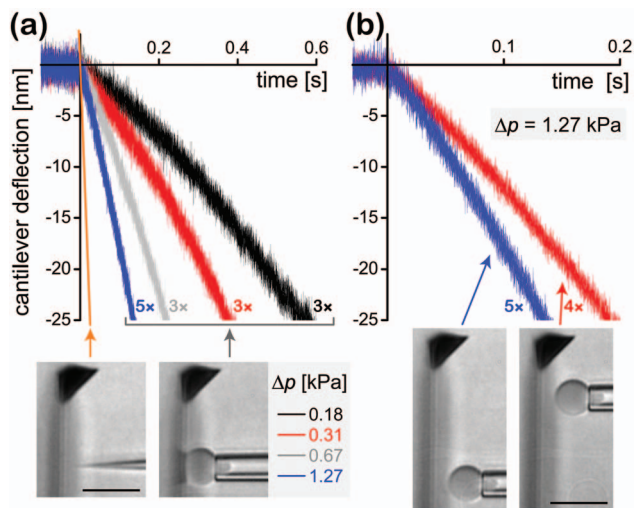


FIG. 2. (Color) Scope and repeatability of the force measurements. Two control parameters were varied between experiments: the pipette-aspiration pressure  $\Delta p$  [(a) the  $\Delta p$ -values are given below the graph] and (b) the contact position along the length of the cantilever. A total of 23 cantilever-deflection curves are shown as a function of time. They were aligned so that the time  $t=0$  corresponded to the moment of first contact between the approaching cell and the stationary cantilever. Nearly indistinguishable results were obtained for each parameter set (three to five individual curves are plotted on top of each other as indicated). Illustrative videomicrographs are included at the bottom (bar= $10\ \mu\text{m}$ ). Note that the recorded cantilever deflection refers to the displacement at the point of cell contact. The conversion from position-detector voltage to cantilever deflection depends on the contact location and had to be separately calibrated for each position. This was done by deflecting the cantilever at each cell-contact position with a rigid needle whose translation speed was precisely known (demonstrated at the lower left).

closed-loop piezoactuator automatically translates the pipette-held red cell to/from the stationary cantilever (see online movie).<sup>13</sup> Custom-written C++/WINDOWS software controls the approach and retraction speeds (kept constant here at  $1\ \mu\text{m/s}$ ) as well as the maximum impingement force and duration of the cell-cantilever contact. To test the assumption that the pressure-dependent, force-deflection be-

havior is the same for different cells (except for a cell-size effect that our analysis accounts for), we have repeated this experiment with seven randomly chosen red blood cells at five to eight different aspiration pressures per cell. Each cell was compressed against the cantilever two to five times at a given pressure. This procedure was carried out at least twice for each cell at different contact positions along the length of the cantilever, amounting to a total of  $\sim 300$  compression cycles. Three cycles were typically repeated under identical conditions (i.e., same cell, aspiration pressure, and cantilever contact position).

A first remarkable outcome of these experiments was their near-perfect repeatability. Without exception, raw data curves (cantilever deflection versus time, Fig. 2) that were recorded under the same conditions exhibited nearly indistinguishable indentation segments, revealing a quick recovery after deformation and, thus, predominantly elastic behavior of the red cells. This is not surprising if one recalls that the human red blood cell is “designed” to cope with numerous recurrent stress situations during its three to four month tenure in the circulation. On the other hand, the observed high sensitivity of the red-cell stiffness to changes in the pipette-aspiration pressure  $\Delta p$  agrees well with expectations. As the cell becomes more pressurized, higher forces are required to deform it, which makes the red cell an easily tunable force transducer.

To compare the experimental results to our theoretical predictions, we converted the raw data curves into graphs of the axial cell indentation  $\Delta D$  [cf. Fig. 1(b)] as a function of the cantilever deflection at the point of cell contact. The example in Fig. 3(a) combines 20 such graphs obtained by repeatedly testing a red blood cell at six different aspiration pressures against the same position of the cantilever. The proper interpretation of the observed nonlinear behavior involves a numerical treatment of the mechanical equilibrium equations of the deformed red blood cell.<sup>8</sup> Inputs to our analysis software are the pipette diameter, the cell’s initial surface area and volume [measured from a video image of the cell held at a low pressure in a pipette, e.g., Fig. 1(d)], the

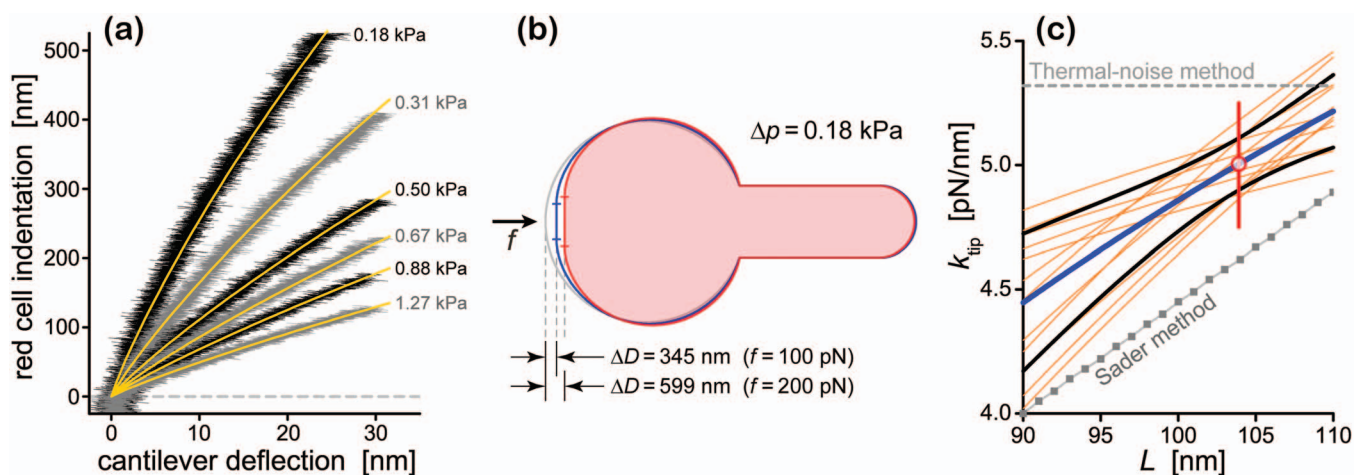


FIG. 3. (Color) Comparison of the measured red-cell deformation with theoretical predictions provides the spring constant of the cantilever. (a) All raw data (cf. Fig. 2) were converted to give the red-cell indentation  $\Delta D$  as a function of the cantilever deflection  $\Delta x_c$ . For each pipette-aspiration pressure  $\Delta p$ , the figure contains at least three nearly indistinguishable graphs, for a total of 20 curves. All six sets of measurements could be well simultaneously matched by our theoretical predictions (bright solid lines) with only one adjustable parameter, the cantilever spring constant  $k(\ell)$ . (b) Examples of numerically computed red-cell contours predicted for the compression experiment of (a). (c) For all measured values of  $k(\ell)$  and  $\ell$ , the tip spring constant  $k_{\text{tip}}$  was calculated as a function of the total cantilever length  $L$  according to (Eq. (1)) thin orange lines. The mean  $k_{\text{tip}}$  values are shown as a thick blue line, flanked by black lines marking the  $\pm\text{SD}$  range. Our ultimate choice of  $k_{\text{tip}}$  (red circle) corresponded to the  $L$  value (vertical red line) that gave the smallest standard deviation. Also shown are the results of other common calibration methods.

area-expansivity modulus of the red-cell membrane [ $\sim 500$  mN/m (Ref. 14)], and the values of the aspiration pressures used. Examples of computed shapes of axially compressed red blood cells are shown in Fig. 3(b). On output, for each pressure  $\Delta p$ , the program stores the predicted cell indentation  $\Delta D$  as a function of the cell-compression force  $f$ . Since  $f$  is also the force required to bend the cantilever, this gives the cantilever deflection as  $\Delta x_c = f/k(\ell)$ , where  $k(\ell)$  is the cantilever spring constant at the position of cell contact (measured in terms of the distance  $\ell$  from the cantilever tip). Thus, the only parameter that is adjustable when *simultaneously* matching the predicted  $\Delta x_c$  values to all measured cantilever deflection curves is the spring constant  $k(\ell)$ . (The program also allows for a small common pressure offset, which always was  $\leq \sim 0.03$  kPa. The offset accounts for shifts of the zero aspiration pressure due to pipette displacements, as well as for the additional small pressure required to overcome the red-cell membrane's shear resistance when forming the cell projection inside the pipette.<sup>15</sup>) Figure 3(a) reveals an excellent global agreement between the six sets of data curves and our theoretical predictions, giving  $k(\ell) = 7.35$  pN/nm in this case.

Finally, to reconcile the results obtained with different cells and at different cantilever positions, we related all measured position-dependent cantilever spring constants  $k(\ell)$  to the respective spring constant at the cantilever tip,  $k_{\text{tip}} \equiv k(0)$ . Simple beam mechanics dictates that for a cantilever with uniform cross section,

$$k_{\text{tip}} = (1 - \ell/L)^3 k(\ell), \quad (1)$$

where  $L$  denotes the full length of the cantilever. Equation (1) shows that  $k_{\text{tip}}$  strongly depends on  $L$ , but unfortunately, the uncertainty in the nominal length given by the manufacturer for the used cantilever is fairly large, with  $L$  ranging between 90 and 110  $\mu\text{m}$ . We also found it difficult to accurately measure  $L$  ourselves because the exact location of cantilever attachment to the AFM chip is hard to visualize on an optical microscope. Instead, we reason that since all measurements should ideally yield the same cantilever-tip spring constant, our best pick for  $L$  is the value that gives the smallest spread in our individual results for  $k_{\text{tip}}$ . Figure 3(c) illustrates how  $L$  is found on this basis. For each trial value of  $L$ , we convert our original measurements of  $k(\ell)$  into  $k_{\text{tip}}$  using Eq. (1) and then evaluate the average and standard deviation of the  $k_{\text{tip}}$  values. Our ultimate tip spring constant corresponds to the value of  $L$ , where the standard deviation is smallest. This approach gave  $L = 103.9$   $\mu\text{m}$ , corresponding to an average spring constant  $k_{\text{tip}} = 5.0$  pN/nm with a standard

deviation of 0.1 pN/nm. Figure 3(c) also includes the spring constants obtained with two other common methods of cantilever calibration. The method of Sader *et al.*<sup>16</sup> gave  $k_{\text{tip}} = 4.6$  pN/nm for the same cantilever, whereas the thermal-noise method<sup>17</sup> yielded  $k_{\text{tip}} = 5.3$  pN/nm. Quite satisfactorily, our value obtained using the red-cell transducers lies midway between the results of the other two calibration methods.

On conclusion, this letter puts forward a rigorous in-depth study of one of the earliest *working* examples of adopting a small natural object or biomaterial to a useful task beyond its natural function, representing a branch of nanobiophysics that is rapidly gaining momentum. The study spans an arc from theoretical membrane physics and numerical analysis, over innovative instrument development and advanced experimentation, to the eventual adaptation of a well-characterized biological object as a device capable of high-resolution nanomechanical measurements. More specifically, we verified the viability of using pipette-aspirated red blood cells as ultrasensitive force-measuring devices. In conjunction with our cantilever-based horizontal force microscope, we were able to vary critical parameters such as the aspiration pressure and the position of cell-cantilever contact and, thus, to carry out a number of self-consistency checks of the utility of the red-cell force transducer. The measurements yielded excellent agreement with our theoretical predictions, proving that among other applications, this transducer can be used to reliably calibrate the spring constants of AFM cantilevers.

<sup>1</sup>E. Evans and K. Ritchie, *Biophys. J.* **72**, 1541 (1997).

<sup>2</sup>G. I. Bell, *Science* **200**, 618 (1978).

<sup>3</sup>P. Nassoy, *Biophys. J.* **93**, 361 (2007).

<sup>4</sup>G. Binnig, C. F. Quate, and C. Gerber, *Phys. Rev. Lett.* **56**, 930 (1986).

<sup>5</sup>E. A. Evans, R. Kwok, and T. McCown, *Cell Biophys.* **2**, 99 (1980).

<sup>6</sup>R. Merkel, P. Nassoy, A. Leung, K. Ritchie, and E. Evans, *Nature (London)* **397**, 50 (1999).

<sup>7</sup>S. Pierrat, F. Brochard-Wyart, and P. Nassoy, *Biophys. J.* **87**, 2855 (2004).

<sup>8</sup>V. Heinrich and C. Ounkomol, *Biophys. J.* **93**, 363 (2007).

<sup>9</sup>C. Ounkomol and V. Heinrich (unpublished).

<sup>10</sup>V. Heinrich and W. Rawicz, *Langmuir* **21**, 1962 (2005).

<sup>11</sup>S. Alexander, L. Hellems, O. Marti, J. Schneir, V. Elings, P. K. Hansma, M. Longmire, and J. Gurley, *J. Appl. Phys.* **65**, 164 (1989).

<sup>12</sup>G. Meyer and N. M. Amer, *Appl. Phys. Lett.* **53**, 1045 (1988).

<sup>13</sup>See EPAPS Document No. E-APPLAB-92-095815 for a movie of a cell compression cycle. This document can be reached through a direct link in the online article's HTML reference section or via the EPAPS homepage <http://www.aip.org/pubservs/epaps.html>.

<sup>14</sup>C. Katnik and R. Waugh, *Biophys. J.* **57**, 877 (1990).

<sup>15</sup>R. Waugh and E. A. Evans, *Biophys. J.* **26**, 115 (1979).

<sup>16</sup>J. E. Sader, J. W. M. Chon, and P. Mulvaney, *Rev. Sci. Instrum.* **70**, 3967 (1999).

<sup>17</sup>J. L. Hutter and J. Bechhoefer, *Rev. Sci. Instrum.* **64**, 1868 (1993).